Heliyon 9 (2023) e22455

Contents lists available at ScienceDirect

Heliyon

journal homepage: www.cell.com/heliyon

A new network representation for time series analysis from the perspective of combinatorial property of ordinal patterns

Yun Lu [a,1], Longxin Yao [b,1], Heng Li [b], Tasleem Kausar [c], Zhen Zhang [a,*], Peng Gao [d], Mingjiang Wang [b,**]

[a] School of Computer Science and Engineering, Huizhou University, Huizhou, Guangdong 516007, China
[b] School of Electronic and Information Engineering, Harbin Institute of Technology, Shenzhen, Shenzhen 518055, China
[c] Mirpur Institute of Technology, Mirpur University of Science and Technology, Mirpur, 10250, AJK, Pakistan
[d] School of Cyber Science and Engineering, Qufu Normal University, Shandong 273165, China

ABSTRACT

Revealing system behavior from observed time series is a fundamental problem worthy of in-depth study and exploration, and has attracted extensive attention in a wide range of fields due to its wide application values. In this paper, we propose a novel network construction method for time series analysis, which is different from the existing ordinal network method concerning the transition probability of ordinal patterns in transition networks. The proposed network representation is based on the combinatorial property concerning the inversion number of ordinal patterns from the ordinal partitions of time series. For the proposed network construction method, the network nodes are represented by each ordinal partition of time series and the edge weight between network nodes is determined by a novel proximity relationship of ordinal patterns which is a newly defined metric based on the inversion number of ordinal patterns. Using random signals and chaotic signals as examples, we demonstrate the potential of the proposed network construction method for the network representation of time series. We also employ the proposed network construction method in quantitative EEG for the identification of three different physiological and pathological brain states. According to the results of *AUC* values, one can observe that the discriminating power of the *AND* of the proposed network construction method is slightly stronger than that of the available ordinal network. The experimental results illustrate that our proposed network construction method opens up a new pathway for network representation of time series, which is capable of quantifying time series for feature extraction and pattern learning for time series analysis.

1. Introduction

The past decade has witnessed a rapid development of complex networks methods for time series analysis [1]. Ranging from natural science to social science, to brain science and so on, the application of complex networks is a very common in many disciplines [2,3]. Transforming a time series into a network domain holds significant practical implications and theoretical significance, which can reveal the dynamics of time series by the study of the resulting network. For instance, McCullough et al. introduced a network measure of ordinal network to quantify the complexity of biological systems, which demonstrated the potential of ordinal network in the analysis of human cardiac dynamics [4]. How to construct a network from observed time series is a fundamental problem worthy of in-depth study and exploration.

In 2006, Zhang and Small introduced the concept of constructing complex networks from pseudo-periodic time series, with each

* Corresponding author.
** Corresponding author.
E-mail addresses: zzsjbme@sjtu.edu.cn (Z. Zhang), mjwang@hit.edu.cn (M. Wang).
[1] Yun Lu and Longxin Yao contributed equally to this work.

https://doi.org/10.1016/j.heliyon.2023.e22455
Received 8 July 2023; Received in revised form 12 November 2023; Accepted 13 November 2023
Available online 20 November 2023
2405-8440/

cycle was represented by a single network node [5]. The approach achieved a transformation from time domain dynamics to network topology, which inspired various methods for analyzing time series from a complex network perspective. These methods include symbolic methods [6], recurrence plots [7], recurrence networks [8], correlation networks [9], etc. The reviews by Donner et al. [10] and Gao et al. [11] provide a comprehensive comparison and summary of methods for analyzing time series from the perspective of complex networks. Overall, transforming time series into complex networks involves two key aspects: mapping time series into network nodes and establishing connections between network nodes based on a specific criterion. Currently, there are three main methods used to construct complex networks for analyzing time series: proximity networks [1], visibility graphs (VG) [12], and transition networks [13]. These methods mainly differ in how they define the network nodes and edges to represent the underlying time series.

The VG method, originally introduced by Lacasa et al. [12], is based on the mutual visibility relationships among successive observations in a scalar time series. Building upon the idea of the natural visibility graph, two variant methods emerged, namely the horizontal HVG [14] and the limited penetrable VG [15]. The transition networks involve mapping a time series into a network representation using symbolic dynamics and transition probabilities of symbolic patterns [13,16]. Typically, the resulting transition network is in the form of a directed weighted network. When analyzing the directed weighted network, it can be regarded as a one-step transition model for system state changes of the underlying time series and interpreted as a Markov chain from a mathematical perspective. The proximity networks, such as recurrence networks [17,18], phase space constructed networks [19], establish a network representation by capturing the similarity or proximity between the trajectories of a dynamical system from the time series. The proximity networks involve mapping individual states to nodes and determining the edges between nodes by examining the relationship between the metrics of the corresponding states for node pairs. As a kind of proximity networks, the most well-established method is the recurrence networks method. Initially introduced by Marwan et al. [7], this method establishes the corresponding relationship between complex networks and time series.

It is noteworthy that proximity networks and transition networks share certain connections with the concept of recurrence. Recurrence of states, in the meaning that states become again arbitrary close to previous ones after some time, is a fundamental property of deterministic dynamical systems. For proximity networks, the connectivity between network node pairs is established through a data-responsive localized way, which is usually achieved by examining the neighborhood regions centered around a specific vertex within either the phase space itself or a given metric space. In this context, a certain (pseudo) distance is employed to access the similarities between their phase points or space states. In contrast, for transition networks, the corresponding space states or classes are rigid, which are usually determined by a fixed coarse-graining of the phase space, ordinal patterns, or other specific related symbolic methods [1]. It should be noted that recurrences can be visualized by recurrence plots (RP) [20], originally introduced by Eckmann et al. [21]. The RP has received close attention in time series analysis and some algorithms have been proposed. Groth proposed the Order Recurrence Plots which was used to visualize dependencies between two time series by applying the concept of cross recurrence plots to the local ordinal structure [20]. Pham et al. introduced fuzzy recurrence plots, which determine an optimal relation between the observed states in phase space and a number of predefined clusters [22].

Among the various network construction methods for time series analysis, the ordinal pattern (OP) based transition networks have gained considerable attention due to their simplicity and computational efficiency [23,24]. This approach offers a simple way of conceptualising a time series to transition networks by means of ordinal partitions from the time series. In Ref. [25], McCullough et al. proposed time lagged ordinal partition networks to characterize the dynamics of time series, which was a generalized version of ordinal partition network based on transition network. In Ref. [26], Kulp et al. used ordinal partition transition networks to analyze ECG signals. In Ref. [13], Pessa et al. used the ordinal networks method to study the characterization of stochastic time series. The OP-based transition networks are inherited from the symbolization approach and the permutation entropy [24]. In this framework, each ordinal pattern is regarded as a network node, and for the symbolized time series, the temporal information of ordinal patterns in succession is to calculate the transition probability, thereby determining the connecting edge relationships.

Worth noting that there are two characteristics (limitations) in the available OP-based transition networks. Firstly, the number of network nodes is solely determined by the number of ordinal patterns, which is unrelated to the actual data points in the time series. To be more specific, the maximum value of network nodes (N) is determined by the embedded dimension d ($N = d!$) [10]. For instance, when the parameter of embedded dimension is set to 3 (that is $d = 3$), the number of ordinal patterns is 6, so the number of network nodes in the OP-based transition networks will be only 6, regardless of the number of the data points of time series. Secondly, according to the definition of transition networks, when two ordinal patterns adjacent in time order appear the same in symbolized time series, the self-loops will appear in the network structure [10]. In the construction of complex networks for time series analysis, it is generally preferred to avoid self-loops as much as possible. This is also evident in previous studies where researchers employed the Kronecker delta function to eliminate self-loops in cycle networks [27], recurrence networks [8,22], correlation networks [9] and so on.

To address these limitations and enhance the flexibility in utilizing ordinal patterns to construct network representations for time series, we propose an innovative network construction method that combines proximity networks with ordinal networks. This novel network representation capitalizes on the combinatorial property of ordinal patterns which effectively combines the fundamental concepts of proximity networks and ordinal partition transition networks that leverage the inversion numbers of ordinal patterns to establish the edge-weight relationships within a network. Unlike the existing OP-based transition networks [12,25,26] that rely on the transition probabilities of ordinal patterns to establish the edge-weight relationship, our proposed network construction method introduces a newly defined metric based on the inversion number of ordinal patterns to establish proximity relationship (pattern similarity) of ordinal patterns in the network representation of time series. In our proposed network construction method, each ordinal partition of the time series represents a network node. As a result, our proposed construction method not only avoids the self-loop structures but also ensures an ample number of network nodes with plentiful connecting edges, facilitating the formation of an informative network topology for time series analysis.

2. Methods

2.1. Inversion numbers for a permutation

The concept of inversions was introduced by G. Cramer in 1750, in connection with his famous rule for solving linear equations [28]. As in mathematics, a permutation of a finite set is an arrangement of its elements into a row. For $d \in \boldsymbol{N}$, we denote the set of all permutations of {0, 1, 2, …, d-1} by $\boldsymbol{\Pi}^d$. Let $(\pi_0, \pi_1, \pi_2, \ldots, \pi_{d\text{-}1}) \in \boldsymbol{\Pi}^d$ where $\pi_i \in \{0, 1, 2, \ldots, d\text{-}1\}$ ($\pi_i \neq \pi_j$ if $i \neq j$) be a permutation of the set {0, 1, 2, …, d-1}. If $i < j$ and $\pi_i > \pi_j$, then the pair (π_i, π_j) is called an inversion of the permutation $(\pi_0, \pi_1, \pi_2, \ldots, \pi_{d\text{-}1})$.

Each inversion is a pair of elements (π_i, π_j) in a permutation that is the right of i that are less than i, and the only permutation with no inversions is the permutation (0 1 2 … d-1) in ascending order. For a given element π_i ($0 \leq i \leq d$-1) in a permutation $\pi = (\pi_0, \ldots, \pi_i, \ldots, \pi_j, \ldots, \pi_{d\text{-}1})$, the number of inversions of element π_i for all pairs (π_i, π_j) (where $i+1 \leq j \leq d$-1) can be calculated and denoted as R_i ($0 \leq i \leq d$-1). More specifically, for the calculation of the inversion number of an element π_i, the R_i can be obtained by counting the number of elements to the right of i that are less than i. By the definition of inversion number, the R_i of element π_i in a permutation will always satisfy the following expression (1):

$$1 \leq R_0 \leq d\text{-}1, 1 \leq R_1 \leq d\text{-}2, 1 \leq R_2 \leq d\text{-}3, \ldots, R_{d\text{-}1} = 0 \tag{1}$$

For example, given a permutation (4 3 1 5 2), the inversion numbers corresponding to each element can be expressed as (2):

$$(3\ \ 2\ \ 0\ \ 1\ \ 0) \tag{2}$$

Because the last elements 3, 1, 2 are less than the first element 4 in permutation (4 3 1 5 2), therefore, the inversion number of the first element in permutation (4 3 1 5 2) is 3. In a similar way, the inversion numbers of the second, third, fourth, and fifth element in the permutation (4 3 1 5 2) are 2, 0, 1, and 0, respectively.

2.2. Ordinal patterns of time series

Considering a general time series composed of N discrete observations, $x = \{x_1, x_2, x_3, \ldots, x_N\}$, when using phase space reconstruction method [29–31], a set of vectors can be reconstructed from the time series $\{x\}$ with embedded dimension d and time lag τ. The resulting vectors in the phase space can be expressed as Equation (3)

$$v_i = \left(x_i, x_{i+\tau}, x_{i+2\tau}, \cdots, x_{i+(d-1)\tau}\right), i = 1, 1+\tau, 1+2\times\tau, \cdots, 1+l\times\tau \tag{3}$$

where $l = \left\lfloor \frac{N}{\tau} \right\rfloor - d + 1$.

According to the values of its d elements, each resulting vector $v_i = (x_i, x_{i+\tau}, x_{i+2\tau}, \ldots, x_{i+(d\text{-}1)\tau})$, can be mapped into one ordinal pattern $O^{(i)} = (\pi_0, \pi_1, \pi_2, \ldots, \pi_{d\text{-}1})$ where $\pi_i \in \{0, 1, 2, \ldots, d\text{-}1\}$ ($\pi_i \neq \pi_j$ if $i \neq j$). More specifically, in order to describe the mapping relationship from vector v_i to ordinal pattern $O^{(i)}$ more intuitively, the indices of the d elements of vector $v_i = (x_i, x_{i+\tau}, x_{i+2\tau}, \ldots, x_{i+(d\text{-}1)\tau})$ are rewritten to $v_i = (x_{i+\pi_0}, x_{i+\pi_1}, x_{i+\pi_2}, \ldots, x_{i+\pi_{d-1}})$ with the d elements of vectors v_i in ascending order, that is

$$x_{i+\pi_0} \leq x_{i+\pi_1} \leq x_{i+\pi_2} \cdots \leq x_{i+\pi_{d-1}}\ ,\ \forall x_{i+\pi_k} \in v_i \ and\ \pi_k = \{0\ ,\ 1\ ,\ 2\ ,\ \cdots\ ,\ d-1\} \tag{4}$$

In Equation (4), it should be noted that if two or more elements of vector v_i are equal ($x_{i+l\text{-}1} = x_{i+l}$), the indices of ordinal pattern for those elements are assigned based on the order of appearance in vector v_i, and can be expressed as the following Equation (5):

$$x_{i+l-1} = x_{i+l} \Leftrightarrow \pi_{l-1} < \pi_l \tag{5}$$

2.3. Ordinal network

Enlightened by the concept of permutation entropy proposed by Bandt and Pompe [24], the ordinal network of time series was proposed by Small et al. [32], which is constructed by the use of the ordinal patterns $O^{(i)} = (\pi_0, \pi_1, \pi_2, \ldots, \pi_{d\text{-}1})$ where $\pi_i \in \{0, 1, 2, \ldots, d\text{-}1\}$. For the construction of ordinal network, all possible permutations for ordinal patterns $O^{(i)} = (\pi_0, \pi_1, \pi_2, \ldots, \pi_{d\text{-}1})$ are regarded as the network nodes, the connections of network nodes are determined by the transition probability of the ordinal patterns $O^{(i)}$ where $i = 1, 2, \ldots, l$ that occurs in temporal succession for time series. Therefore, the edges of the ordinal network are directional according to the temporal succession of ordinal patterns $O^{(i)}$ and $O^{(i+1)}$. The edge weight of ordinal network is defined as the relative frequency in which the temporal succession $(O^{(i)}, O^{(j)})$ occurs, and the elements of weight matrix for ordinal network of time series can be expressed as Equation (6):

$$p_{i,j} = \frac{\text{number of times}\ \ O^{(i)} \text{followed by}\ \ O^{(j)}}{M} \tag{6}$$

where $i, j = 1, 2, \ldots, d!$ and the denominator M represents the total number of ordinal pattern transitions.

For the available ordinal network, to construct a network representation for time series, the data points required are usually relatively large, because according to the formation way of network nodes, the nodes are corresponding to all the possible permutations for ordinal patterns $O^{(i)} = (\pi_0, \pi_1, \pi_2, \ldots, \pi_{d\text{-}1})$ where $\pi_i \in \{0, 1, 2, \ldots, d\text{-}1\}$ and $i = 1, 2, \ldots, l$. When the value of the embedding dimension d is larger, the network nodes of the constructed ordinal network will become much greater in number ($d!$). Besides, for the existing ordinal network when the ordinal patterns, occurring in temporal succession of the ordinal partitions of time series, are the same, there may be some self-loops in the network structure. The self-loop structures are useless, which are usually discarded during complex network analysis.

2.4. *Defining ordinal pattern number to quantify the similarity of ordinal pattern*

According to the above facts, we can know that for time series, $x = \{x_1, x_2, x_3, \ldots, x_N\}$, the ordinal pattern $O^{(i)} = (\pi_0, \pi_1, \pi_2, \ldots, \pi_{d\text{-}1})$ is essentially a permutation in the permutation set of $\{0, 1, 2, \ldots, d\text{-}1\}$, that is $O^{(i)} \in \boldsymbol{\Pi}^d$. From the perspective of the combinatorial property of ordinal pattern, based on the inversion number of permutation, we define a metric for quantifying the ordinal patterns. The metric is referred as ordinal pattern number (*OPN)*, and its expression is defined as follows

$$OPN\left(O^{(i)}\right) = Inv(\pi_0) \times \left(R_{0,MAX}\right)! + Inv(\pi_1) \times \left(R_{1,MAX}\right)! + \cdots + Inv(\pi_{d-1}) \times \left(R_{d-1,MAX}\right)! + 1 \quad (7)$$

where $(\cdot)!$ is the factorial function, $R_{i,MAX}$ is corresponding to the maximum value of the inversion number of the element π_i in the permutation $\pi = (\pi_0, \pi_1, \pi_2, \ldots, \pi_{d\text{-}1})$, and $Inv(\pi_i)$ represents the inverse number of each element π_i in the ordinal pattern $O^{(i)}$. Based on Equation (4), $R_{0,MAX} = d\text{-}1$, $R_{1,MAX} = d\text{-}2$, $R_{3,MAX} = d\text{-}3$, etc., and it is well-known that for d-1 objects in mathematics there will be $(d\text{-}1)!$ permutations. Hence, the factorial function is applied in Equation (7), and Equation (7) can be reduced to

$$OPN\left(O^{(i)}\right) = Inv(\pi_0) \times (d-1)! + Inv(\pi_1) \times (d-2)! + \cdots + Inv(\pi_{d-2}) \times (1)! + 1 \quad (8)$$

According to Equation (8), the minimum value of *OPN* is 1, corresponding to the permutation $\pi = (0, 1, 2, \ldots, d\text{-}1)$ in ascending order; and the maximum value of *OPN* is $d!$, corresponding to the permutation $\pi = (d\text{-}1, \ldots, 2, 1, 0)$ in descending order.

To determine the similarity of ordinal patterns, the *OPNs* of ordinal patterns are further exploited. Given that any two ordinal patterns (permutations) $O^{(k)} \in \boldsymbol{\Pi}^d$ and $O^{(v)} \in \boldsymbol{\Pi}^d$, the pattern similarity degree (*PSD*) of ordinal patterns between $O^{(k)}$ and $O^{(v)}$ can be quantified based on the value of *OPN* for the ordinal partitions. It is important to note that the *PSD* denote the similarity calculation value of any two ordinal patterns $O^{(k)}$ and $O^{(v)}$, and it is essentially a two-dimensional array. The definition of $PSD(O^{(k)}, O^{(v)})$ can be expressed as follows

$$PSD\left(O^{(k)}, O^{(v)}\right) = \left|OPN\left(O^{(k)}\right) - OPN\left(O^{(v)}\right)\right| \quad (9)$$

where $|\cdot|$ is the absolute value function. According to Equations (8) and (9), the minimum value of $PSD(O^{(k)}, O^{(v)})$ is 0, which indicates that the two ordinal patterns are the same, and the maximum value of $PSD(O^{(k)}, O^{(v)})$ is $(d!\text{-}1)$, which indicates that the two ordinal patterns are of maximal difference between each other. When two ordinal patterns are more similar, the value of $PSD(O^{(k)}, O^{(v)})$ will be closer to 0, which is somewhat similar to the neighborhood relation of the Order Recurrence Plot proposed by Groth [20]. The Order Recurrence Plot is originally used as a visualization tool to quantify the coupling strength between two time series based on the local ordinal structure. It needs to be emphasized that there are two main differences between the proposed $PSD(O^{(k)}, O^{(v)})$ and Order Recurrence Plot. For one thing, the $PSD(O^{(k)}, O^{(v)})$ is used for a single time series and the Order Recurrence Plots is mainly used for two

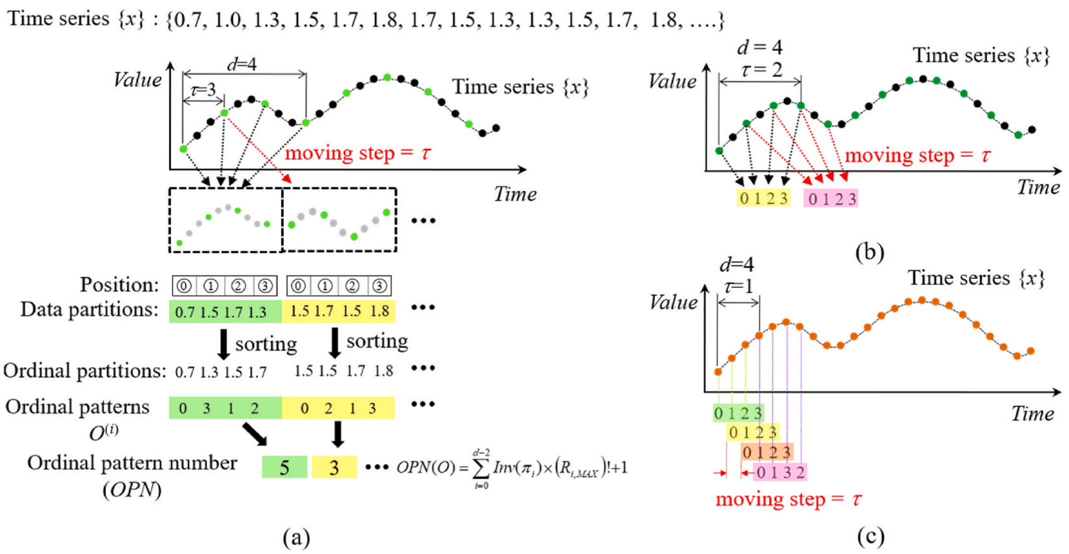

Fig. 1. Schematic diagram of the mapping process from time series to ordinal patterns of network nodes by the use of phase space reconstruction method with a fixed embedded dimension $d = 4$ and four kinds of time lags (a) $\tau = 3$, (b) $\tau = 2$, (c) $\tau = 1$.

time series. For another, the concept of $PSD(O^{(k)}, O^{(v)})$ can establish multi-level metrics for quantifying various ordinal patterns, but for the Order Recurrence Plot, the recurrence of order patterns is defined as the neighboring if their order patterns coincide, which is essentially a binary quantization of various ordinal patterns. Consequently, in our work, the concept of *PSD* defined above can be better used to quantify the similarity of ordinal patterns for analyzing single time series.

2.5. Proposed network construction method for time series

In this paper, a new network construction method for time series is proposed, which exploits the inversion numbers of ordinal patterns from the perspective of combinatorial property of permutation to establish the edge-weight relationship in a network. Fig. 1 shows the schematic diagram of the mapping process from time series to ordinal patterns of network nodes in a network. Given a time series $\{x\} = \{0.7, 1.0, 1.3, 1.5, 1.7, 1.8, 1.7, 1.5, 1.3, 1.3, 1.5, 1.7, 1.8, \ldots\cdot\}$, using phase space reconstruction with embedded dimension $d = 4$ and different time lags τ=3, 2 and 1 as shown in Fig. 1(a)–(c), a series of ordinal patterns $O^{(i)}$ where $i = 1, 2, \ldots, l$ is obtained from the ordinal partitions of time series in succession. As network node representation, each ordinal partition of time series is treated as one node associated with a specific ordinal pattern that actually corresponds to a permutation. According to Equation (8), the corresponding *OPN* of ordinal patterns of network nodes can be calculated, and the neighboring relationship of any two network nodes is quantified by Equation (9). Therefore, the network edges representing the connected relationship can be determined by the *PSD* for the corresponding ordinal patterns.

In order to illustrate the calculation procedure of the proposed network construction method, the basic flow of network representation of time series is presented in Fig. 2(a). For the proposed network construction method, there are three main calculation processes as shown in Fig. 2(a): 1) Each ordinal partition obtained from time series $\{x\}$ is treated as a network node, and the *OPN* of the corresponding ordinal patterns can be calculated according to Equation (7); 2) Next, taking advantage of the calculation results of *OPN* with Equation (8), the PSD matrix can be calculated for any node pairs (ordinal partitions), which is corresponding to the edge weights between node pairs in the network; 3) Sequentially, using a PSD threshold selection algorithm to determine a threshold parameter T, the adjacency matrix and the connections of nodes can be calculated from the resulting PSD matrix.

It is important to state that in this paper, our work focus on the construction of unweighted network for time series. Hence, the resulting adjacency matrix can represent all the network information of an unweighted network. By exploiting the criterion of the network connectivity with the parameter scanning of threshold T, the adjacency matrix representing an unweighted network with the edge connectivity is calculated from the resulting PSD matrix. The parameter of PSD threshold T is determined according to the minimum number of edges required to make the network connected, and the pseudocode implementation of the calculation of the PSD threshold T and adjacency matrix for unweighted network representation is shown in Fig. 2(b).

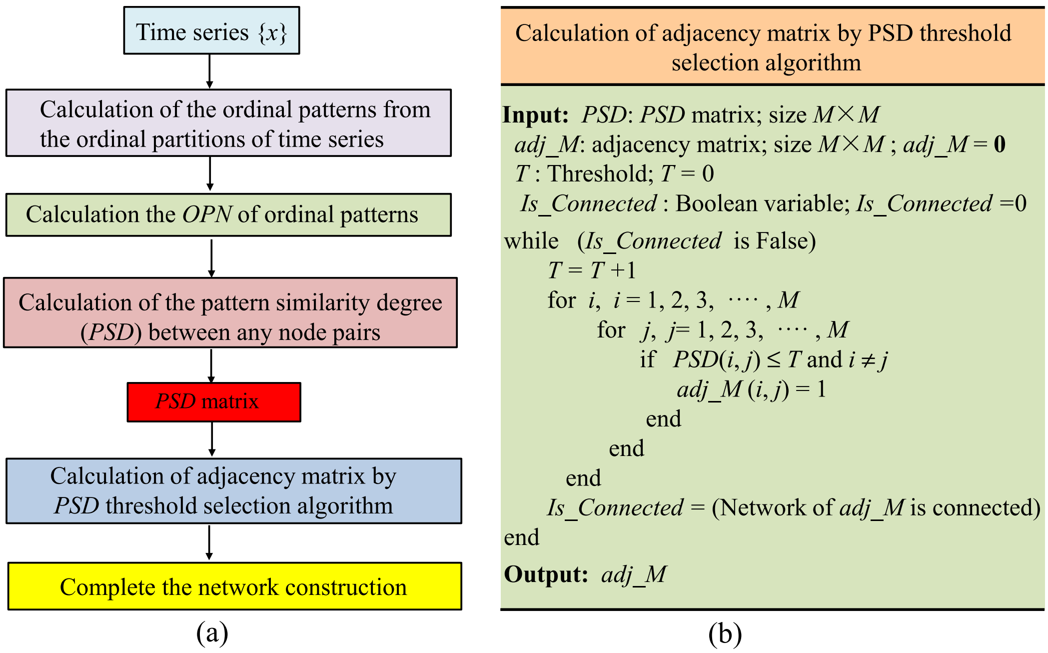

Fig. 2. (a) Calculation flow of the proposed network construction method from time series; (b) Pseudocode implementation of the calculation of adjacency matrix by PSD threshold selection algorithm.

2.6. Network measures for performance evaluation

A network can be represented as a graph $G = (V, E)$, where V is the set of network nodes (vertices), and E is the set of network edges [12]. There are two important matrices related to a network, adjacency matrix and weight matrix, which are often used to denote the topological structure of networks. For a network having N nodes, the weights of the network edges are represented as a weight matrix $\boldsymbol{W}$. Similarly, adjacency matrix also contains important information about the links present of all network nodes. However, when the types of complex networks are different, there is a little difference between the two matrices. Unlike weighted complex network, the elements of adjacency matrix and weight matrix for unweighted complex network have a unit value if there is a connection edge between any node pairs [1]. In addition, it is worth noting that an unweighted complex network can be constructed by applying a proper threshold T to the elements of the weight matrix of its weighted counterpart [1].

In our paper, the clustering coefficient (CC) and average node degree (AND) are used to measure the properties of a network. The AND of a network with M nodes can capture the local properties of a network and is defined as the mean value of summation of degree of all nodes in a network [33], as expressed in Equation (10):

$$AND = \frac{1}{M}\sum_{i=1}^{M} dgr(i) \tag{10}$$

where $dgr(i)$ is the degree of node i.

The ACC can measure the mean value of how many neighbors of a node are also neighbors of each other [33], which is the fraction of connecting neighbor nodes averaged over the whole network, as expressed in Equation (11):

$$ACC = \frac{1}{M} \times \sum_{i\in M, \forall m_i} \frac{2e_{p,q}}{n_{m_i} \times (n_{m_i} - 1)}, \quad p, q \in V_{m_i}, \ e_{pq} \in E \tag{11}$$

where m_i is the number of one-hop neighbor nodes, $e_{p,q}$ is the one-hop connection between neighbor node p and neighbor node q, $n_{m_i} \times (n_{m_i} - 1)$ denotes the possible number of links that can be formed among n_{m_i} neighbor nodes.

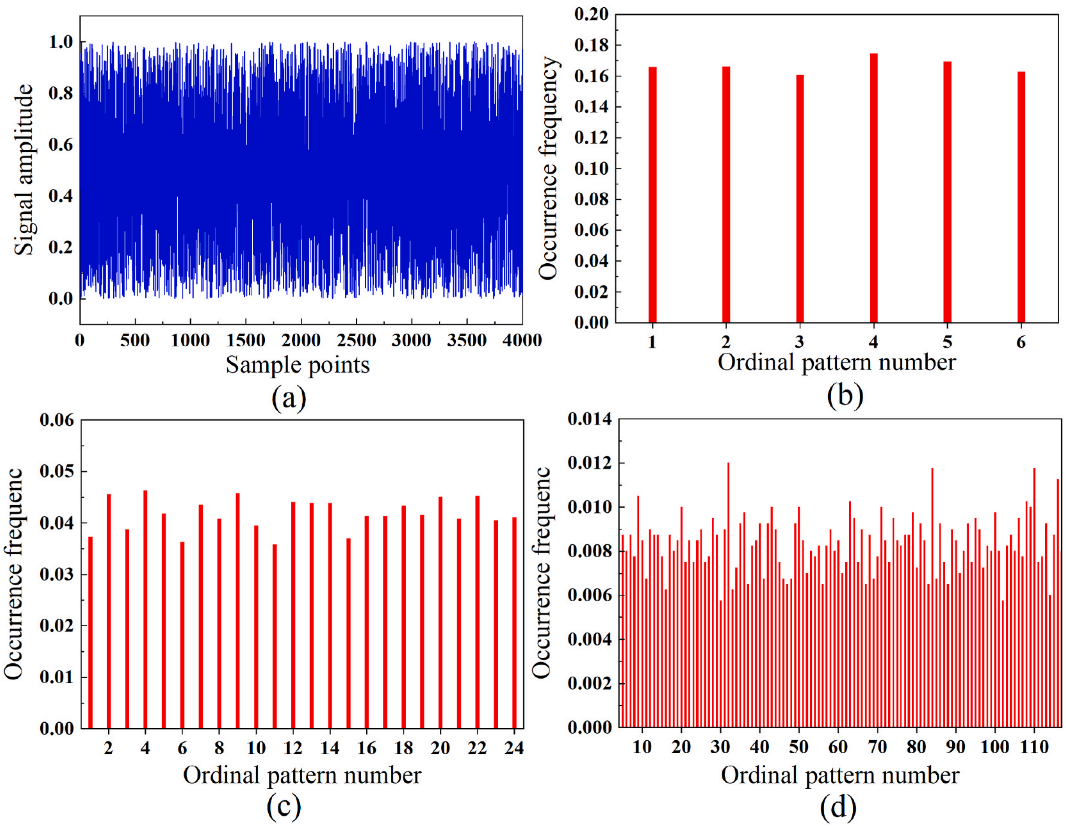

Fig. 3. The ordinal patterns statistics of network representation from random signals by the proposed network construction method. (a) An example of random time series; (b) Occurrence frequency of ordinal patterns with embedded dimension $d = 3$; (c) Occurrence frequency of ordinal patterns with embedded dimension $d = 4$; (d) Occurrence frequency of ordinal patterns with embedded dimension $d = 5$. The time lag τ is fixed as 1.

3. Results

To demonstrate the proposed network construction method for time series, we firstly use numerically generated time series with known properties to start our empirical investigation. In our study, two types of numerically simulate signals (random signals, chaotic signals) are investigated, which are recognized as good approximations of many real-world data [34]. In addition, we further use our proposed network construction method to characterize EEG signals, so as to illustrate its application potential.

3.1. Results for the network construction from random signals

Random time series are sequences of serially uncorrelated random variables. In our experiment, the random signals used are uniformly distributed pseudo-random numbers in the interval (0, 1). Fig. 3(a) presents an example of random time series used in our experiment, which consists of 4000 samples (data points). For our proposed complex networks method to construct networks from random signals, the scalar time series are first reconstructed into a series of ordinal partitions based on phase space reconstruction method using different embedded dimension d with a fixed time lag $\tau = 1$. According to the definition of the proposed network construction method, each one of ordinal partitions is regarded as a network node, which is with a kind of ordinal patterns. When the embedded dimension d is 3, 4, and 5, the number of these types of ordinal patterns is 6, 24, and 120, respectively. Fig. 3(b)–(d) present the statistical results of the occurrence frequency of the ordinal patterns for the network construction from random signals. It is noted that when the embedded dimension $d = 3$, 4, and 5, the total numbers of ordinal patterns (ordinal partitions or network nodes) from random signals consisting of 4000 samples are 3996, 3995, and 3994, respectively. As shown in Fig. 3(b), for the embedded dimension $d = 3$, the occurrence frequency of ordinal patterns exhibits an approximately equal probability.

For Fig. 3(c)–(d), the results of the occurrence frequencies of ordinal patterns seem to be different from that of Fig. 3(b). This is mainly due to the statistical deviation of ordinal patterns. Because the values of embedded dimension d of Fig. 3(c)–(d) are greater than that of Fig. 3 (b), the total number of ordinal patterns will vary greatly. For Fig. 3(b), the total number of ordinal patterns is 6; For Fig. 3 (c) and (d), the total numbers of ordinal patterns are 24 and 120, respectively. However, the number of data points of random signals has a fixed length (4000 points), this will certainly bring some statistical deviation for the ordinal pattern statistics with respect to the different total number of ordinal patterns. If the data points of random signals can be as long as possible, the results of the occurrence frequencies of ordinal patterns of Fig. 3(c)–(d) can show consistency.

For our proposed network construction method, the PSD matrix is very important index to quantify the ordinal patterns with the aim to determine the network edges of the constructed networks from random signals. In order to reveal the PSD matrices of arbitrary

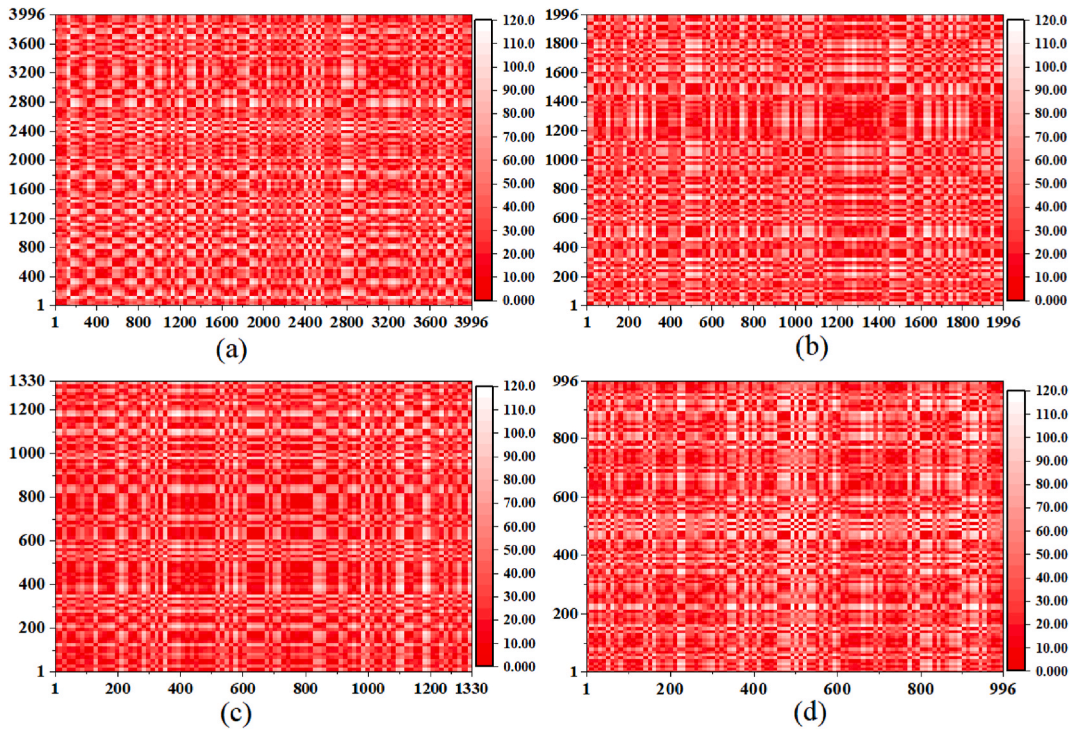

Fig. 4. The PSD matrices of the network representation from random signals by the proposed network construction method using a fixed embedded dimension $d = 5$ with different time lags (a) $\tau = 1$; (b) $\tau = 2$; (c) $\tau = 3$; (d) $\tau = 4$. The white-and-red textures indicate the degree of similarity in ordinal patterns associated with any node pairs in the constructed networks, and the maximum value of 120 for the white-and-red textures corresponds to the factorial of embedded dimension ($d = 5$).

network nodes for the proposed network construction method, the network construction from random signals of 4000 samples, using a fixed embedded dimension $d = 5$ and different time lags, are investigated in the experiment. Fig. 4 presents the experimental results for the PSD matrix of the network construction from random signals based on phase space reconstruction method with a fixed embedded dimension $d = 5$ and four kinds of time lag ($\tau = 1$, 2, 3, and 4, which are corresponding to Fig. 4(a), (b), (c) and (d), respectively). It is noted that when the embedded dimension is fixed to $d = 5$, the total numbers of network nodes (ordinal partitions) from random signals consisting of 4000 samples are 3996, 1996, 1330, and 996, respectively.

For the random signals of 4000 samples to construct a network using a fixed embedded dimension $d = 5$, the PSD matrix with the context of the white-and-red textures in Fig. 4, denotes the degree of similarity in ordinal patterns that are associated with each of node pairs in the constructed network. Because the embedded dimension d is set to 5, the value of the white-and-red texture is from 0 to 120, which represent the values of elements in PSD matrix. According to the definition of PSD, the smaller the values of PSD elements are, the more similar the ordinal pattern of network node pairs are, showing in Fig. 4 that the white-and-red textures deepen in red color. It should be noted that although the white-and-red textures of the anti-diagonal elements (from left bottom side to right upper side) in PSD matrix in Fig. 4 are red, it has no specific meaning about the similarity of ordinal patterns, because it corresponds to the node itself.

To obtain an unweighted network, based on the adaptive threshold method for the PSD elements, the PSD matrix can be easily transformed into a binary matrix, which is corresponding to the adjacency matrix of the constructed unweighted network from random signals. In the experiment, a classic criterion is used, which gradually increases the PSD threshold from the initial zero so that makes the constructed network from random signals change from disconnected to connected network, and the resulting critical value is selected as the target PSD threshold to construct an unweighted network. Fig. 5 shows the experimental results for the adjacency matrices of the unweighted network construction from random signals of 4000 samples. This network construction is based on phase space reconstruction method using a fixed embedded dimension $d = 5$ with different time lags $\tau = 1$, 2, 3, and 4, corresponding to Fig. 5 (a), (b), (c), and (d), respectively. As shown in Fig. 5, the red color textures contain information about the connected edges in the constructed networks, and the connections between arbitrary nodes in the constructed networks is with random and uniform characteristics.

3.2. *Results for the network construction from Lorenz signals*

In order to further demonstrate the reliable use of the proposed network construction method for time series analysis, the network

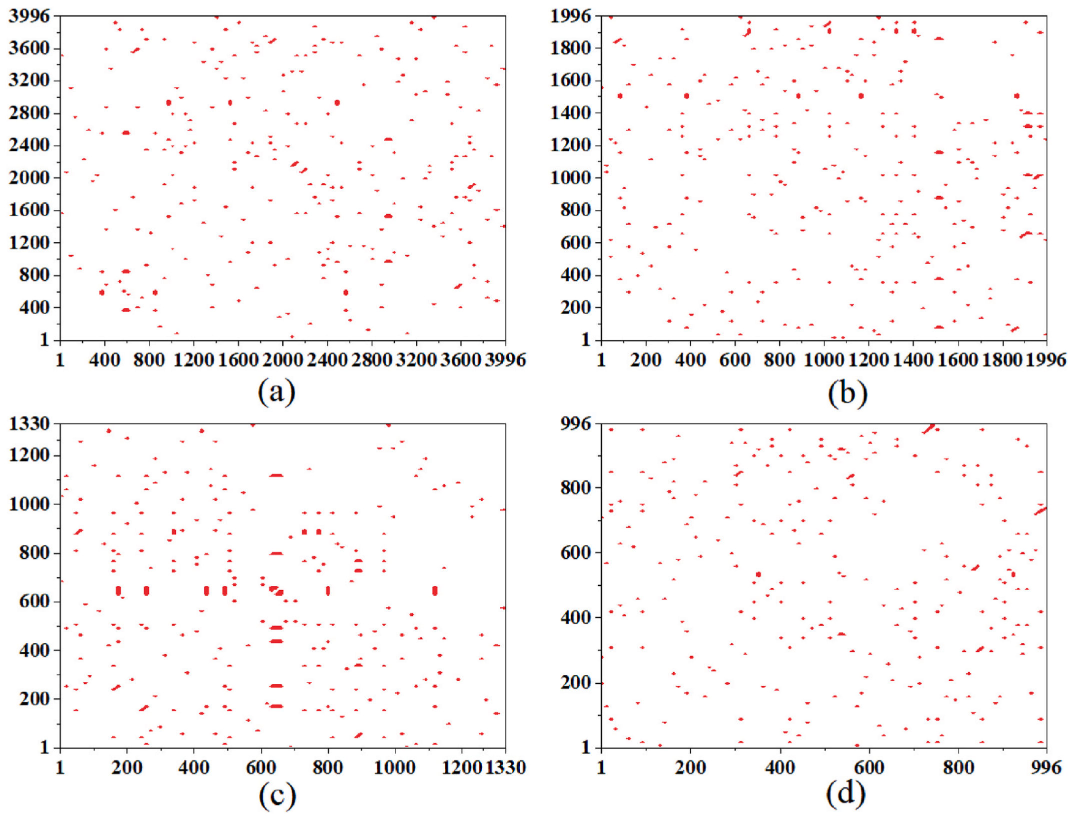

Fig. 5. The adjacency matrices of the network construction from random signals by the proposed network construction method using a fixed embedded dimension $d = 5$ with different time lags (a) $\tau = 1$; (b) $\tau = 2$; (c) $\tau = 3$; (d) $\tau = 4$. The red color textures contain information about the connected edges present in the constructed network from random signals.

construction of chaotic signals is investigated. In our experiment, the simulate chaotic signals are generated based on a Lorenz system, the system function of which is expressed in Equation (12). According to Equation (12), the x, y and z components can be obtained, which is corresponding to the convection velocity, temperature difference, and temperature gradient components, respectively. Fig. 6 (a) presents an example of x component of Lorenz system used in our experiment, which consists of 2000 samples.

$$\begin{cases} \frac{dx}{dt} = -10\times(x-y) \\ \frac{dy}{dt} = 30\times x - y - x\times z \\ \frac{dz}{dt} = x\times y - \frac{8}{3}\times z \end{cases} \tag{12}$$

Similar to random signals, in order to study the statistical characteristic of the ordinal patterns from x component of Lorenz system, the network constructions from the x component are constructed using the different embedded dimension $d = 3$, 4, and 5, respectively, with a fixed time lag $\tau = 1$. Fig. 6(b)–(d) present the statistical results of the occurrence frequency of the ordinal patterns for the network construction from x component of Lorenz system, which are corresponding to the embedded dimension $d = 3$, 4, and 5, respectively. It should be noted that for Fig. 6(b)–(d), the total number of occurrence frequency statistics of ordinal patterns is 1996, 1995 and 1994 respectively, because the number of data points is 2000, time lag τ is fixed as 1, and the embedded dimension d is set to 3, 4, and 5. As shown in Fig. 6(b)–(d), for a given value of d, the occurrence frequency of ordinal patterns exhibits a distinct feature. More specifically, the occurrence frequency for the largest value and the smallest value of *OPN* is significantly higher than the other ordinal patterns. It is worth noting that the statistical results of occurrence frequency of the ordinal patterns for Lorenz signals exhibit obvious pattern characteristic.

In order to reveal the PSD matrices of arbitrary network nodes, the network structure from Lorenz system x component of 2000 samples, using a fixed embedded dimension $d = 5$ and different time lags, are investigated in the experiment. Fig. 7 presents the experimental results for the PSD matrix of the network construction from x component of Lorenz system. This network construction is based on phase space reconstruction method with a fixed embedded dimension $d = 5$ and four kinds of time lags $\tau = 1$, 2, 3, and 4,

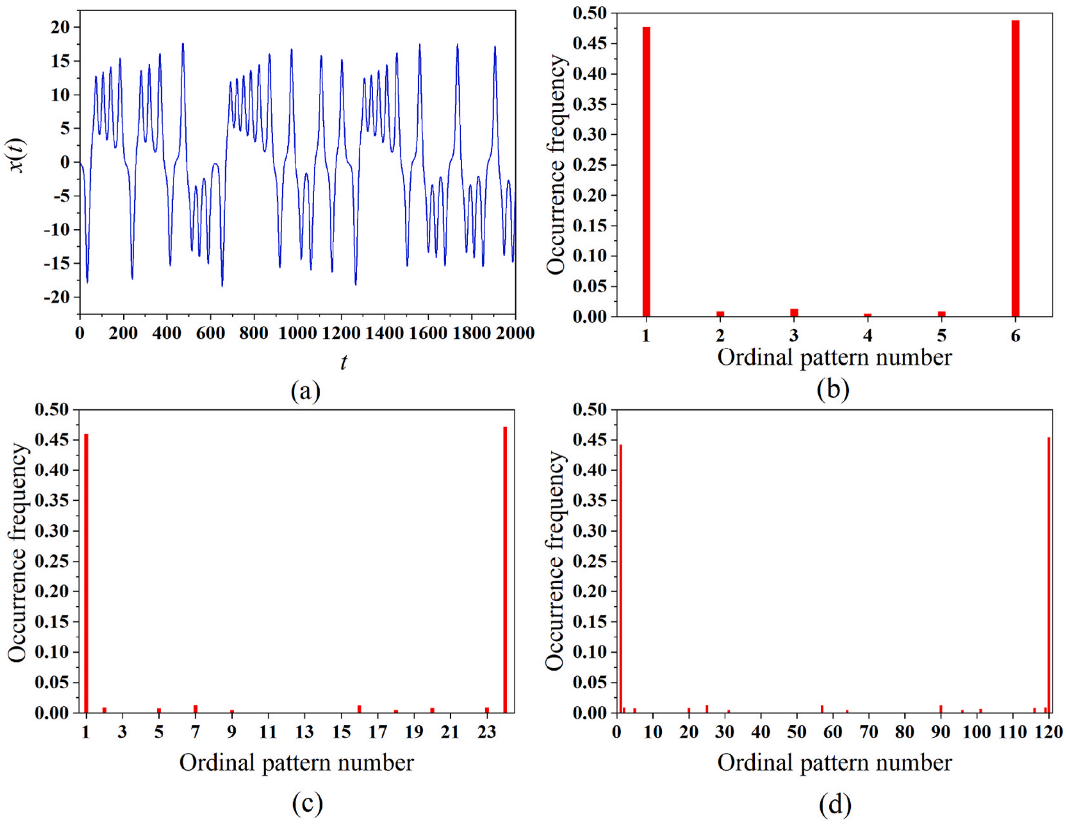

Fig. 6. The ordinal patterns statistics of the network representation from the x component of Lorenz system by the proposed network construction method. (a) An example of x component of Lorenz system; (b) Occurrence frequency of ordinal patterns with embedded dimension $d = 3$; (c) Occurrence frequency of ordinal patterns with embedded dimension $d = 4$; (d) Occurrence frequency of ordinal patterns with embedded dimension $d = 5$. The time lag τ is fixed as 1.

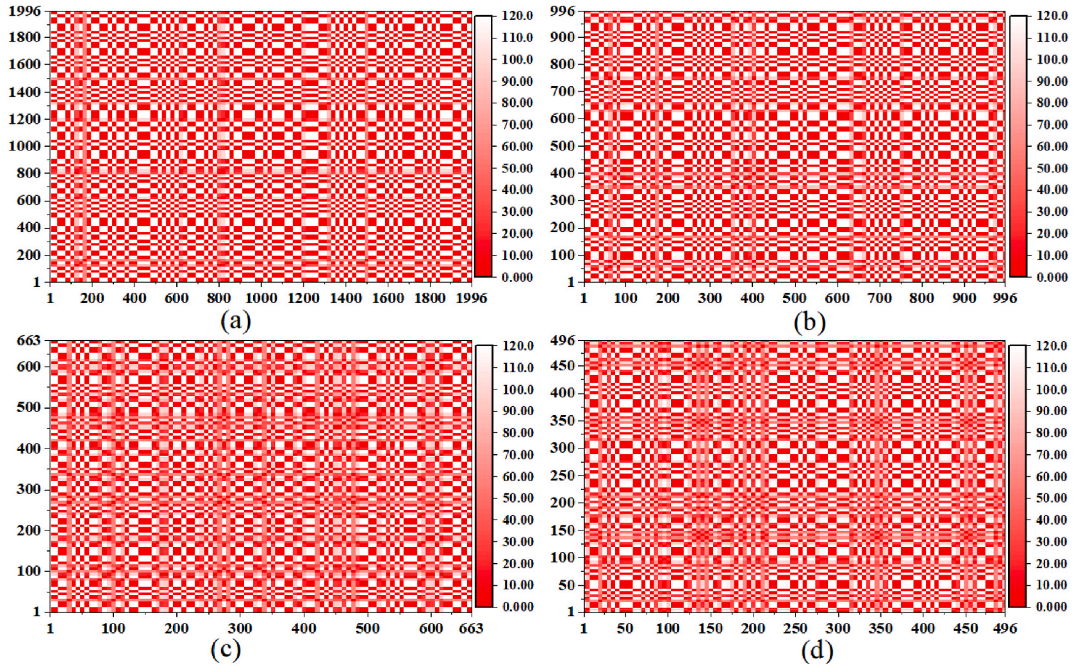

Fig. 7. The PSD matrices of the network representation from the x component of Lorenz system by the proposed network construction method using a fixed embedded dimension $d = 5$ with different time lags (a) $\tau = 1$; (b) $\tau = 2$; (c) $\tau = 3$; (d) $\tau = 4$. The white-and-red patterns indicate the degree of similarity in ordinal patterns associated with any node pairs in the constructed networks, and the maximum value of 120 for the white-and-red texture corresponds to the factorial of embedded dimension ($d = 5$).

corresponding to Fig. 7(a), (b), (c), and (d), respectively. It should be noted that when the embedded dimension is fixed to $d = 5$, the total numbers of network nodes (ordinal partitions) from the x component of Lorenz system consisting of 2000 samples are 1996, 996, 663, and 496, respectively.

As shown in Fig. 7, when constructing a network for the x component of Lorenz system with a fixed embedded dimension $d = 5$, the PSD matrix, characterized by white-and-red textures, indicates the degree of similarity in ordinal patterns that are associated with each pair of nodes in the constructed network. Similar to random signals, according to the definition of PSD, the smaller the values of PSD elements are, the more similar the ordinal pattern of network node pairs are. This is evident in Fig. 7, where the white-and-red textures deepen in red color, indicating a higher degree of similarity.

To obtain an unweighted network, similar to random signals processing methods, based on adaptive threshold method, the PSD matrix is transformed into an adjacency matrix of the constructed unweighted network from the x component of Lorenz system. Fig. 8 (a)-(d) show the experimental results for the adjacency matrix of the unweighted network construction from Lorenz x component of 2000 samples, based on phase space reconstruction method using a fixed embedded dimension $d = 5$ with different time lags $\tau = 1$, 2, 3, and 4, respectively. As shown in Fig. 8, the red color textures contain information about the edges present in the constructed networks from x component of Lorenz system.

3.3. Results for the network construction from EEG signals

To demonstrate the application potential for the proposed network construction method in practice, the network construction of EEG signals which were collected from brain electrical activity from different physiological and pathological brain states and from different recording regions [35], is investigated. The EEG dataset has been widely studied in the research community, and it contains 5 data subsets (Sets A-E), and each of which contains 100 single channel EEG recordings of 23.6-sec duration (4097 samples) that were recorded with the same 128-channel amplifier system. In our experiment, EEG signals of three data subsets (Sets C, D, and E) are used to perform the network construction and analysis by the proposed network construction method, which are corresponding to three different physiological and pathological brain states.

More specifically, the EEG signals of Set C are from non-focus side during seizure free intervals. The EEG signals of Set D are from epileptic focus during seizure free intervals. The EEG signals of Set E correspond to seizure activity from sites exhibiting ictal activity. For the EEG signals of 4097 samples to construct a network based on embedded dimension $d = 6$ and $\tau = 2$ by the use of our proposed network construction method, and the PSD matrices of size 2044×2044 can be easily obtained. By the use of adaptive threshold method to the PSD matrices, an unweighted network is then constructed from EEG signals. Fig. 9 shows three examples of unweighted networks derived from EEG signals of three different physiological and pathological brain states. The resulting adjacency matrices, depicted in Fig. 9(a), (b), and (c), characterize the three EEG-related brain states corresponding to non-focus side during seizure free

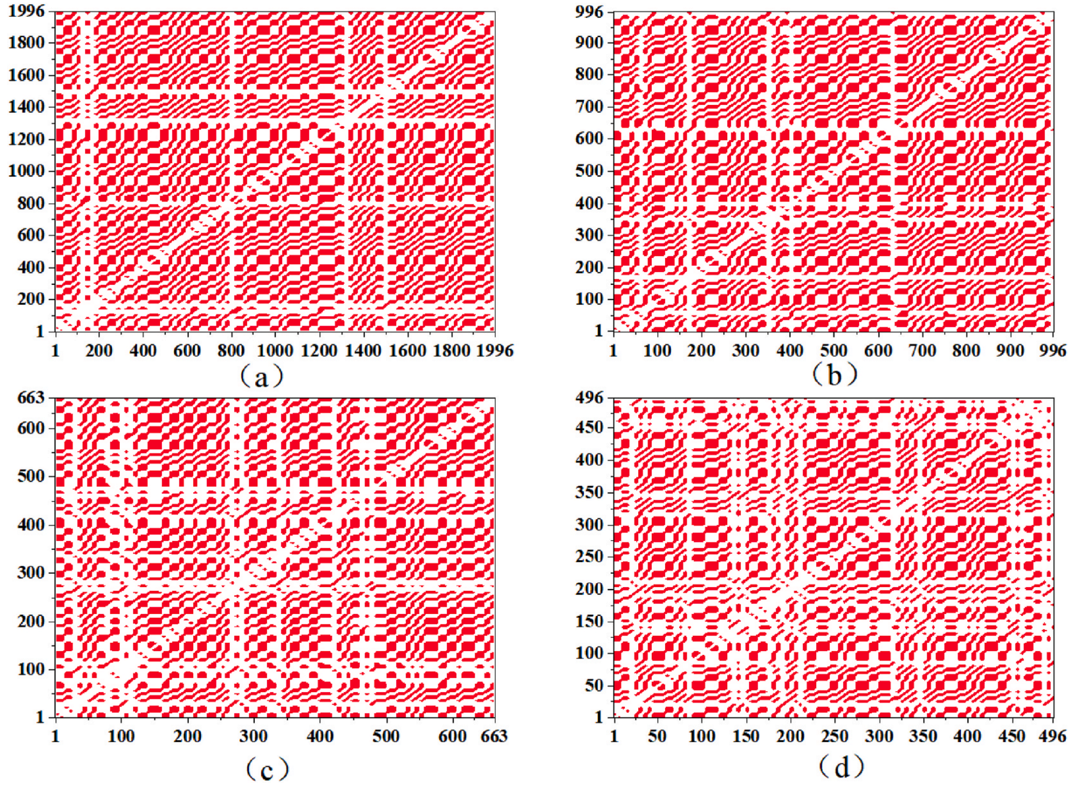

Fig. 8. The adjacency matrices of the constructed network from the x component of Lorenz system by the proposed network construction method using a fixed embedded dimension $d = 5$ with different time lags (a) $\tau = 1$; (b) $\tau = 2$; (c) $\tau = 3$; (d) $\tau = 4$. The red color texture contains information about the edges present in the constructed network from the x component of Lorenz system.

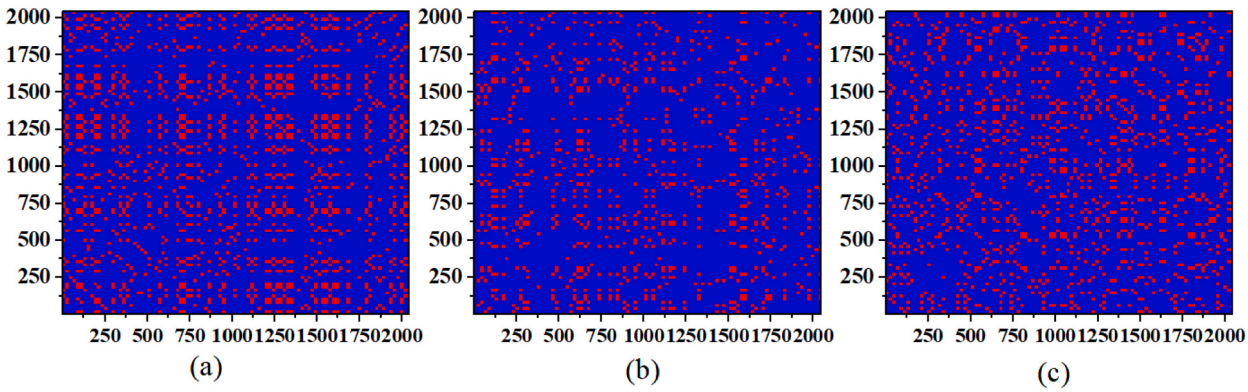

Fig. 9. Three examples of unweighted networks from EEG signals of three different physiological and pathological Brain States (A, B and C) by the proposed network construction method. (a) Adjacency matrix to Brain State A; (b) Adjacency matrix to Brain State B; (c) Adjacency matrix to Brain State C. Brain State A: correspond to EEG signals from non-focus side during seizure free intervals; Brain State B: correspond to EEG signals from epileptic focus during seizure free intervals; Brain State C: correspond to EEG signals from epileptic focus during seizure activity. The red color textures indicate the connection information of the edges in the constructed networks.

intervals, epileptic focus during seizure free intervals, epileptic focus during seizure activity, respectively, the red color textures of which indicate the connection information of the edges in the constructed networks.

In order to reveal the power of the unweighted networks constructed from EEG signals, in our experiment two kinds of popular network measures, *CC* and *AND*, are further extracted from the constructed unweighted networks. To analyze the discriminating power of network measure of EEG signals, the receiver operating characteristic (ROC) curve and AUC (area under the ROC curve) are used to assess the performance for the classification of three different physiological and pathological brain states based on the metrics, *CC* and *AND*. An ROC curve can show the performance of a classification model at all classification thresholds. In our experiment, to better

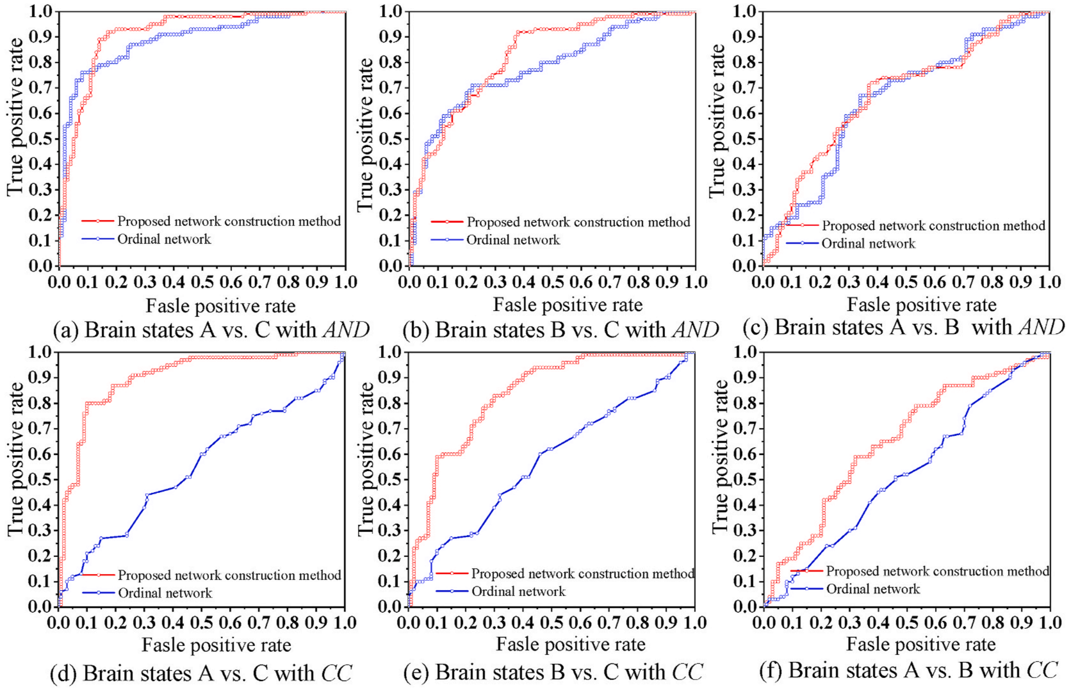

Fig. 10. ROC curves for the classification of three different physiological and pathological Brain States (A, B and C) with the network measures of *AND*, *CC* by the proposed network construction method and the available ordinal network. (a) Brain States A vs C with *AND*; (b) Brain States B vs C with *AND*; (c) Brain States A vs B with *AND*; (d) Brain States A vs C with *CC*; (e) Brain States B vs C with *CC*; (f) Brain States A vs B with *CC*.

reveal the discriminative power of the network measures based on the constructed network, a native binary classification model is used to classify the input features of *CC* and *AND* based on a given feature threshold. More specifically, when the instances larger than the threshold are considered to be one class (positive instance), and the instances smaller than the threshold are considered to be the other class (negative instance).

The ROC curve is created by plotting the true positive rate (*TPR*) against the false positive rate (*FPR*) at different classification thresholds [36,37]. The *TPR* is calculated as $TP/(TP + FN)$, where *TP* is the number of true positives and *FN* is the number of false negatives. The *TPR* is the probability that an actual positive will test positive. The *FPR* is calculated as $FP/(FP + TN)$, where *FP* is the number of false positives and *TN* is the number of true negatives. The *FPR* is the probability that a true positive will be missed by the test. Fig. 10(a)-(c) presents the ROC curves for the classification of three different physiological and pathological brain states with the *AND* and *CC* of the constructed networks from the EEG signals. To convincingly illustrate the performance difference of network representations for time series, an ordinal network published in the year 2019 [13] was selected as the baseline method, and used to compare with our proposed network construction method.

According to the ROC curve, the area under the ROC (*AUC*) can be calculated. As shown in Fig. 10(a)–(c), for the classification between the Brain States A vs. C, Brain States B vs. C, and Brain States A vs B, with the network measure of *AND*, the *AUC* values are 0.9126 and 0.8886, 0.8228 and 0.7784, 0.6711 and 0.6559, which are corresponding to the proposed network construction method and the available ordinal network, respectively. In Fig. 10(d)–(f), for the classification between the Brain States A vs. C, Brain States B vs. C, and Brain States A vs B, with the network measure of *CC*, the *AUC* values are 0.9002 and 0.5504, 0.8322 and 0.5706, 0.6499 and 0.5232, corresponding to the proposed network construction method and the available ordinal network, respectively. For the classification of three different physiological and pathological Brain States (A, B and C), the larger the value of *AUC*, the stronger the discriminating power of the corresponding network measure.

Therefore, according to the results of *AUC* values, one can observe that the discriminating power of the *AND* of the proposed network construction method is slightly stronger than that of the ordinal network, but the discriminating power of the *CC* of the proposed network construction method is much stronger than that of the ordinal network. For the *CC* network measure, the reason why the performance of the ordinal network is so weak may be that the number of EEG data points is not enough. For the construction of an ordinal network, a large embedding dimension usually requires a large number of the data points for time series [13]. If the data points of time series are not large enough, the network structure in ordinal network may be very sparse, which may lead to insufficient characterization of the dynamic property of EEG signals.

4. Discussion

When exploring the transformation of time series into networks, two primary considerations are the methods for forming network nodes and determining edge weights. For our proposed network construction method, it combines two common network representation core concepts of proximity networks and ordinal networks. As a kind of classical transition networks, ordinal network for time series network representation was first proposed by Small [32]. For an ordinal network, with a process of mapping the temporal succession of ordinal partitions of time series into a Markov chain to obtain a network representation [13], the edge weight is determined based on the transition probabilities concerning the temporal information of the ordinal patterns for time series. However, from the perspective of the combinatorial property ordinal patterns, our proposed network representation method of time series can be regarded as a generalization of ordinal networks, and the edge weight of the proposed network representation method is determined by a proximity relationship of ordinal patterns that is a newly defined metric based on the inversion number of ordinal patterns.

There are several distinctions between our proposed network construction method and the existing ordinal network. First, the establishment of edge weight is one of the biggest differences between the two network construction methods. For the proposed network construction method, based on the ordinal partitions from time series with the characteristics of permutation and combination, the edge weight of the constructed network is quantified based on the *PSD* value of ordinal patterns associated with the corresponding network nodes. However, For the existing ordinal network, the transition probabilities of ordinal patterns are used to establish the edge weight. Second, the formation way of network nodes is also obvious different. Our proposed network construction method is based on the ordinal partitions of time series, but for the existing ordinal network each ordinal pattern of time series is treated as one network node. Thirdly, there are notable disparities in the types and structures of the networks constructed from time series between our proposed method and the existing approach. For the existing ordinal network, the constructed network is directional, and usually has self-loop structures. However, for our proposed network construction method, the constructed network is nondirectional, and no self-loop structure.

Due to these differences mentioned above, our proposed network construction method shows a significant advantage compared to the existing ordinal network. For the existing ordinal network, the size of the network nodes is mainly determined by the embedding dimension d with respect to the phase space reconstruction, which does not depend directly on the data points of time series. The network nodes of the existing ordinal network are defined by the ordinal patterns associated with the ordinal partitions of time series, the total number of which is the factorial of the embedding dimension ($d!$). When the value of the embedding dimension d is larger, the network nodes of the constructed ordinal network will become much greater in number ($d!$). For a network representation with a large number of nodes, if the data points of time series are not large enough, the network structure may be very sparse, which may lead to insufficient characterization of the dynamic property of time series. Fig. 11 shows the curve of the embedding dimension d versus the number of all possible ordinal patterns (network nodes).

As shown in Fig. 11, when the embedding dimension d is 9, the number of all possible ordinal patterns is 362,880. When the number of time series points is much lower than this, the constructed ordinal network may be very sparse. However, for our proposed network construction method, the size of the network nodes is determined by ordinal partitions of time series. As the network nodes of the two network construction methods exhibit varying dependencies on the embedding dimension of phase space reconstruction, our proposed network construction method has a clear advantage in that it requires a smaller number of time series points to construct the network compared to the existing ordinal network.

To go a step further, to convincingly illustrate the performance difference of network representations for time series with different network construction methods, we perform some comparative experiments and analysis using our proposed network construction method and an available ordinal network. The available ordinal network using for characterizing stochastic time series published in the year 2019 [13] was selected as the baseline method. To ensure fair comparison, our proposed network construction method and the baseline method are investigated under the same algorithm parameters of phase space construction. Using the logistic map, we examine the performance difference of our proposed network construction method and the baseline method. For the two network construction methods, the algorithm parameters of phase space construction are set to be embedded dimension $d = 5$ and time lag $\tau = 1$. Mathematically, the logistic map is written as the following Equation (5):

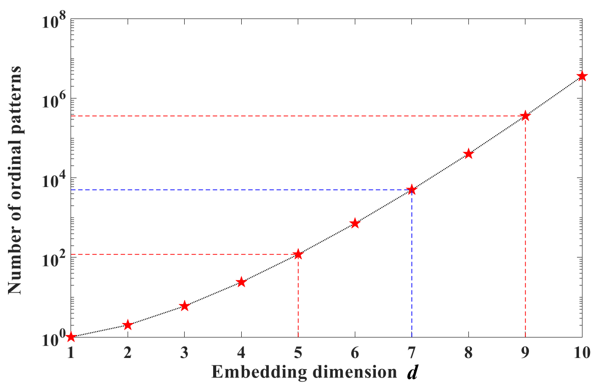

Fig. 11. Curve of the embedding dimension d versus the number of all possible ordinal patterns (network nodes) for the existing order network of time series.

$$x_{i+1} = r \times x_i \times (1 - x_i) \tag{13}$$

where x_i is a number between zero and one, and r is a control parameter. The logistic map represents a recurrence relation, and chaotic behavior can arise from the non-linear dynamical equation as shown above. We first conduct experimental analysis using a logistic sequence of 1000 points. In the experiment, within the interesting range of the control parameter $r \in [3.5, 4]$ with a step size of $\Delta r = 0.0005$ [7], the dynamic regimes and transitions of the chaotic behavior for the logistic sequence can be plotted. The bifurcation diagram of the logistic map is presented in Fig. 12(a). Fig. 12(b) and (c) present the average node degree (*AND*) of network representation from the logistic map over the different control parameter r, which are corresponding to our proposed network construction method and the baseline method (ordinal network), respectively.

According to the results shown in Fig. 12(b) and (c), one can be observed that for our proposed network construction method and the baseline method, the values of *AND* can indicate the dynamic region and transition of the logistic map, which demonstrate the dynamic information embedded in the network structures. Besides, the values of the *AND* of our proposed network construction method are much greater than those of the baseline method (ordinal network). Hence, compared to the existing ordinal network, the network constructed by our proposed method has a more densely network connections, which may be more robust in network structure. In addition, it should be noted that with respect to the dependency of the values of *AND* on the control parameter r, our proposed network construction method is different from the baseline method. This is mainly because of the difference of the connected edge definition between our proposed network construction method and the baseline method. Meanwhile, this phenomenon further reveals that our proposed network construction method is a new network representation, which is different from the existing methods.

In practical application, similarly to the available ordinal network, the embedding dimension d and time lag τ are two important parameters for the proposed network construction method, which have crucial impacts on the appearance of order patterns. To obtain the ordinal patterns, time series must first be reconstructed in phase space with the two parameters. As recommended in Ref. [1], the range of $5 \leq d \leq 10$ is most useful when using common network measures to characterize the dynamics of time series. Compared with the embedding dimension d, there are several traditional criteria to determine whether the selection of the time lag τ is appropriate. In general, the time lag τ may be appropriate when the statistical correlation between the vectors in the phase space is close to zero. Therefore, it is a possible way to select the time lag τ according to the value of time lag τ corresponding to the first root of the autocorrelation function of time series [25]. In addition, using the first minimum of the time-delayed mutual information (MI) to determine the time lag τ is also a common method [38].

For demonstration purposes, we utilize the mutual information method to determine the selection of time lag τ for network representation by experiment on real EEG. In the experiment, two EEG signals are randomly selected the data subsets Set D and E mentioned in subsection 3.3. Fig. 13 shows the relationship between the mutual information of the EEG signals over the parameter of time lag τ. As shown in Fig. 13(a) and (b), based on the first minimum of the time-delayed mutual information, for the proposed network construction method, the values of time lag τ are determined to be 16 and 4, corresponding to the EEG signals from Set D and Set E, respectively.

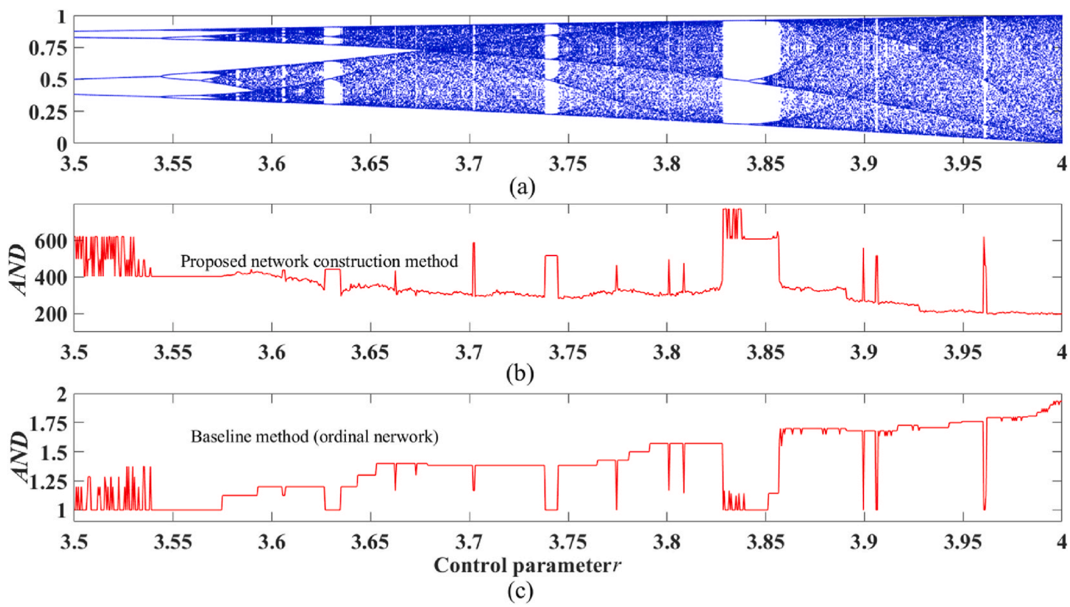

Fig. 12. (a) Bifurcation diagram of the logistic map; (b) *AND* of the network representation from the logistic map by the proposed network method; (c) *AND* of the network representation from the baseline method (ordinal network).

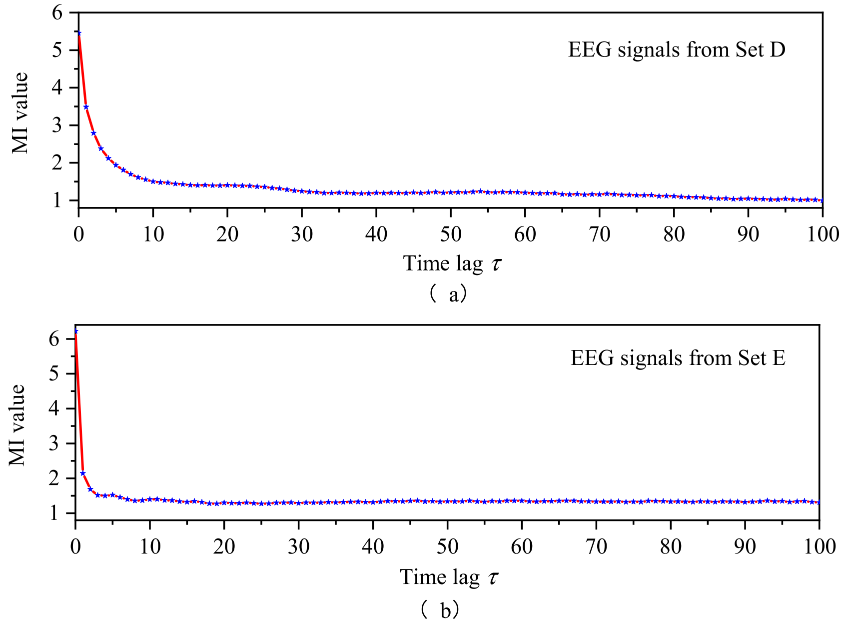

Fig. 13. Using the first minimum of the time-delayed mutual information of EEG signals to select time lag τ. (a) Time lag τ corresponding to EEG signals from Set D is selected to 16 for the proposed network construction method; (b) Time lag τ corresponding to EEG signals from Set E is selected to 4.

5. Conclusions

In this paper, we propose an innovative network construction method from time series by exploiting the combinatorial property of ordinal patterns. We first give the main approach and basic definition of network construction from a mathematical point of view, and the specific mathematical formulas are introduced to determine the pattern similarity degree of network nodes, which are used to establish the connection relationship of network edges. Then, we illustrate the process of constructing networks from time series using our proposed network construction method by applying it to two common types of time series, namely random and chaotic signals, as examples. Finally, using real EEG signals, our experiment further demonstrates the application potential of the proposed network construction method for the classification of three different physiological and pathological brain states. We are convinced that our proposed network construction method establishes a new pathway for network representation of time series, which is capable of quantifying time series in the application fields of feature extraction and pattern learning. In the future work, we will further study how to adaptively determine the parameters (embedded dimension, time lag) for network construction. Additionally, we aim to refine the selection of network metrics in practical use from the perspective of the basic rationales of complex network construction.

Funding

This work was supported in part by the National Natural Science Foundation of China (No. 62176102), the Guangdong Basic and Applied Research Foundation under Grant 2020A151511049, the fund which aims to improve scientific research capability of key construction disciplines in Guangdong province (No: 2022ZDJS058), and [the Young Project of GuangDong Basic and Applied Basic Research Foundation] grant number [2022A1515110138].

Data availability statement

Data associated with the study will be made available on request.

CRediT authorship contribution statement

Yun Lu: Writing – review & editing, Writing – original draft. **Longxin Yao:** Writing – review & editing, Data curation. **Heng Li:** Investigation, Data curation. **Tasleem Kausar:** Validation, Formal analysis, Data curation. **Zhen Zhang:** Writing – review & editing, Conceptualization. **Peng Gao:** Writing – review & editing, Data curation. **Mingjiang Wang:** Supervision, Conceptualization.

Declaration of competing interest

The authors declare that they have no known competing financial interests or personal relationships that could have appeared to influence the work reported in this paper.

References

[1] Z. Yong, R.V. Donner, N. Marwan, J.F. Donges, J. Kurths, Complex network approaches to nonlinear time series analysis, Phys. Rep. 787 (2018) 1–97.
[2] Zhiyuan Yang, Ya Chen, Xinle Hou, Yun Xu, Feng Bai, Topologically convergent and divergent large scale complex networks among Alzheimer's disease spectrum patients: a systematic review, Heliyon 9 (4) (2023), e15389.
[3] Hengguo Luo, Banking systemic risk estimating of China's banking industry during the COVID-19 pandemic—based on complex network theory, Heliyon 8 (11) (2022), e11391.
[4] M. McCullough, M. Small, H.H.C. Iu, T. Stemler, Multiscale ordinal network analysis of human cardiac dynamics, Phil. Trans. Roy. Soc. Lond. 375 (2096) (2017), 20160292.
[5] J. Zhang, M. Small, Complex network from pseudoperiodic time series: topology versus dynamics, Phys. Rev. Lett. 96 (23) (2006), 238701.
[6] P. Li, B.H. Wang, Extracting hidden fluctuation patterns of hang seng stock index from network topologies, Phys. Stat. Mech. Appl. 378 (2) (2007) 519–526.
[7] N. Marwan, J.F. Donges, Y. Zou, R.V. Donner, J. Kurths, Complex network approach for recurrence analysis of time series, Phys. Lett. 373 (46) (2009) 4246–4254.
[8] T.D. Pham, From fuzzy recurrence plots to scalable recurrence networks of time series, Europhys. Lett. 118 (2) (2017), 20003.
[9] Y. Yang, H. Yang, Complex network-based time series analysis, Phys. Stat. Mech. Appl. 387 (5–6) (2008) 1381–1386.
[10] R.V. Donner, M. Small, J.F. Donges, N. Marwan, Y. Zou, R. Xiang, J. Kurths, Recurrence-based time series analysis by means of complex network methods, International Journal of Bifurcation and Chaos 21 (4) (2011) 1019–1046.
[11] Z.K. Gao, M. Small, J. Kurths, Complex network analysis of time series, Europhys. Lett. 116 (5) (2016), 50001.
[12] L. Lacasa, B. Luque, F. Ballesteros, J. Luque, J.C. Nuño, From time series to complex networks: the visibility graph, Proc. Natl. Acad. Sci. U.S.A. 105 (13) (2008) 4972–4975.
[13] A.A.B. Pessa, H.V. Ribeiro, Characterizing stochastic time series with ordinal networks, Phys. Rev. 100 (4) (2019), 042304.
[14] B. Luque, L. Lacasa, F. Ballesteros, et al., Horizontal visibility graphs: exact results for random time series, Phys. Rev. 80 (4) (2009), 046103.
[15] T.T. Zhou, N.D. Jin, Z.K. Gao, et al., Limited penetrable visibility graph for establishing complex network from time series, Acta Phys. Sin. 61 (3) (2012), 030506.
[16] J. Zhang, J. Zhou, M. Tang, H. Guo, M. Small, Y. Zou, Constructing ordinal partition transition networks from multivariate time series, Sci. Rep. 7 (1) (2017) 7795.
[17] T.D. Pham, Fuzzy weighted recurrence networks of time series, Phys. Stat. Mech. Appl. 513 (2018) 409–417.
[18] T.D. Pham, Quantification analysis of fuzzy recurrence plots, Europhys. Lett. 137 (6) (2022), 62002.
[19] Z. Gao, N. Jin, Complex network from time series based on phase space reconstruction, Chaos 19 (3) (2009), 033137.
[20] A. Groth, Visualization of coupling in time series by order recurrence plots, Phys. Rev. 72 (4) (2005), 046220.
[21] J.P. Eckmann, S.O. Kamphorst, D. Ruelle, Recurrence plots of dynamical systems, Europhys. Lett. 4 (9) (1987) 973–977.
[22] T.D. Pham, Fuzzy recurrence plots. Fuzzy recurrence plots, Europhys. Lett. 116 (5) (2016), 50008.
[23] X. Liu, Z. Fu, A novel recognition strategy for epilepsy EEG signals based on conditional entropy of ordinal patterns, Entropy 22 (10) (2020) 1092.
[24] C. Bandt, B. Pompe, Permutation entropy: a natural complexity measure for time series, Phys. Rev. Lett. 88 (17) (2002), 174102.
[25] M. McCullough, M. Small, T. Stemler, H.H.C. Iu, Time lagged ordinal partition networks for capturing dynamics of continuous dynamical systems, Chaos 25 (2015), 053101.
[26] C.W. Kulp, J.M. Chobot, H.R. Freitas, G.D. Sprechini, Using ordinal partition transition networks to analyze ECG data, Chaos 26 (7) (2016), 073114.
[27] J. Zhang, J. Sun, X. Luo, K. Zhang, T. Nakamura, M. Small, Characterizing pseudoperiodic time series through the complex network approach, Phys. Nonlinear Phenom. 237 (22) (2008) 2856–2865.
[28] D.E. Knuth, The Art of Computer Programming, Pearson Education, 1997.
[29] D. Cuesta-Frau, Using the information provided by forbidden ordinal patterns in permutation entropy to reinforce time series discrimination capabilities, Entropy 22 (5) (2020) 494.
[30] M. Zanin, A. Rodríguez-González, E. Menasalvas Ruiz, D. Papo, Assessing time series reversibility through permutation patterns, Entropy 20 (9) (2018) 665.
[31] T. Gutjahr, K. Keller, Generalized ordinal patterns and the KS-entropy, Entropy 23 (8) (2021) 1097.
[32] M. Small, Complex networks from time series: capturing dynamics, in: Proceedings of the 2013 IEEE International Symposium on Circuits and Systems, (ISCAS), 2013, pp. 2509–2512, 19-23 May 2013.
[33] B.S. Manoj, A. Chakraborty, R. Singh (Eds.), Complex Networks: A Networking and Signal Processing Perspective, Pearson, 2018.
[34] T.D. Pham, Time-shift multiscale entropy analysis of physiological signals, Entropy 19 (6) (2017) 257.
[35] R.G. Andrzejak, K. Lehnertz, F. Mormann, C. Rieke, P. David, C.E. Elger, Indications of nonlinear deterministic and finite-dimensional structures in time series of brain electrical activity: dependence on recording region and brain state, Phys. Rev. E: Stat., Nonlinear, Soft Matter Phys. 64 (6) (2001), 061907.
[36] M. Majnik, Z. Bosnić, ROC analysis of classifiers in machine learning: a survey, Intell. Data Anal. 17 (3) (2013) 531–558.
[37] A.P. Bradley, The use of the area under the ROC curve in the evaluation of machine learning algorithms, Pattern Recogn. 30 (7) (1997) 1145–1159.
[38] A.M. Fraser, H.L. Swinney, Independent coordinates for strange attractors from mutual information, Phys. Rev. 33 (2) (1986) 1134–1140.